Chapter 8

Quaternary Faulting on the Fatigue Wash Fault

By Jeffrey A. Coe, John Oswald, Giovanni Vadurro, and Scott C. Lundstrom

Contents

Abstract 111
Introduction and Setting 111
Methods 112
Measurement of Scarp Profiles 112
Logging of Trenches 112
Results 112
Scarp Profiles 112
Stratigraphy, Soils, and Age Constraints in Trenches CF1 and CF1A 112
Structure Exposed in Trenches CF1 and CF1A 118
Paleoseismic Interpretations from Trench Data 119
Event Z 119
Event Y 119
Event X 122
Event W 122
Event V 122
Pre-Event V Deformation 122
Paleoseismic Interpretations from Scarp Data 122
Slip Rates and Recurrence Intervals 124
Faulting and Volcanism 124
Acknowledgments 124

Abstract

Studies of trenches excavated across the south-central section of the Fatigue Wash Fault in Crater Flat, and of scarp profiles near the trenches, provide evidence for five or more surface-rupturing paleoearthquakes on the fault since the middle Pleistocene. Trenches CF1 and CF1A expose a 3-m-thick sequence of alluvial gravel, colluvial wedges, eolian silt, and at least two well-developed silica- and carbonate-cemented soils. The main fault in trench CF1 ranges from 0.35 to 1.40 m in width and is characterized by two fissure fills and a carbonate-engulfed shear zone. The presence of basaltic ash in the youngest colluvial wedge and fissure fill indicates that one Quaternary faulting event correlates with an eruption of the nearby Lathrop Wells volcanic center at 77±6 ka.

Questionable fracturing of surficial deposits as young as 9±1 ka represents the most recent paleoseismic event (Z) on the Fatigue Wash Fault. A 20- to 40-cm offset on a surficial deposit with a minimum age of 17 ka may also have occurred during event Z. Penultimate event Y, which postdates the Lathrop Wells eruption, may be as young as 38±4 ka, whereas the next-older event (X) is dated by the eruption. Vertical displacement ranges from 18 to 35 cm for event Y and from 25 to 42 cm for event X. Event W predates the eruption but is dated at <102+42/−15 ka; displacement was 35 to 63 cm. One or more earlier faulting events that are also evident in trench exposures may be older than 400 ka.

Cumulative displacements measured on scarps formed in surficial deposits dated at older than 400 ka range from 1.3 to 2.8 m, indicating a long-term slip rate of 0.003 to 0.007 mm/yr on the Fatigue Wash Fault. Cumulative vertical displacement resulting from the four most recent faulting events (W–Z) in trench exposures is approximately 1.4 m but only 0.4 m after correction for local tilting of trench units. Net cumulative displacement, taking into account the tilting of surficial deposits and a strike-slip component of movement, is 0.6 m. That much offset within the past 102+42/−15 k.y. indicates an average slip rate of 0.004 to 0.007 mm/yr. Recurrence intervals range from 30 to 140 k.y. for the four latest faulting events.

Introduction and Setting

The Fatigue Wash Fault is a down-to-the-west, dip- to oblique-slip fault about 2.5 km west of the west edge of the proposed repository site for the storage of high-level radioactive wastes at Yucca Mountain (see chap. 3; fig. 2). To the northwest, the fault lies at the base of the prominent west flank of Jet Ridge before terminating near the prow of Yucca Mountain (Scott and Bonk, 1984; Simonds and others, 1995; Day and others, 1998b). The fault bifurcates about the midpoint of Jet Ridge to form a saddle in West Ridge. The splay that cuts West Ridge connects with the Windy Wash Fault on the west side of West Ridge. To the south, the Fatigue Wash Fault continues along the east edge of Crater Flat and appears to merge with the Southern Windy Wash Fault just south of trenches CF2 and CF3 (fig. 2). Quaternary slip along the Fatigue Wash Fault has been documented in alluvial gravel deposits between its south and north intersections with the Windy Wash Fault (Simonds and others, 1995). Slickensides on bedrock fault planes range in rake from 14° to 70° (Scott and Bonk, 1984; Simonds and others, 1995). Slip indicators in Quaternary deposits were not observed.

In the early 1980s, trench CF1 (fig. 2) was excavated across a prominent west-facing scarp in surficial gravel along the central section of the Fatigue Wash Fault. The trench was oriented perpendicular to the fault on the sideslope of a modern channel, and Swadley and Hoover (1983) and Swadley and others (1984) provided a log of the principal stratigraphic and soil relations on the north wall. In 1992, trench CF1 was deepened about 1 m, and a shallow trench (CF1A, fig. 35) was excavated about 10 m to the south to expose the youngest units along the fault that had been disturbed or removed during the excavation of trench CF1. In 1995, scarp profiles were measured near both trenches and at localities to the north where the fault cuts lower to upper Pleistocene alluvium. This chapter summarizes the Quaternary paleoseismic history of the fault as interpreted from scarp profiles and detailed logs of exposures in trenches CF1 and CF1A, and supersedes a preliminary interpretation by Coe and others (1995).

Methods

Measurement of Scarp Profiles

A total of seven topographic profiles (SP1–SP7, table 24) were measured across the west-facing scarp of the Fatigue Wash Fault near trench CF1 (fig. 35): five (SP1–SP5) on the unit 1 surface (fig. 35), one (SP6) on the units 1–3 surface, and one (SP7) on the units 3–4 surface. Six of the profiles (SP1–SP6) were measured by using an electronic surveying instrument (total station), and one profile (SP7) was measured by hand, using a measuring tape and hand level. Measurements of scarp height, surface offset, and maximum scarp-slope angle were calculated from plots of these profiles according to the methodology and nomenclature (fig. 36) of Bucknam and Anderson (1979) and Machette (1989).

Logging of Trenches

Trenches were logged by field and close-range photogrammetric methods (see chap. 1 for details) in 1994. Lithologic units were described by using standard sedimentologic terminology, and soil-horizon descriptions follow the nomenclature of Birkeland (1984) and Machette (1985). Paleoearthquakes were identified on the basis of offset units across the fault, colluvial wedges or fault fissures, and the upward termination of fractures. U-series and thermoluminescence analyses were used to date lithologic units, soil horizons, and surface ruptures. Dating methods are described in chapter 2, and estimated ages of samples collected in the trenches are listed in table 23.

Results

Scarp Profiles

The seven scarp profiles (SP1–SP7) measured along the Fatigue Wash Fault are shown in figures 37*A* through 37*G*, respectively, and surface offsets and scarp heights are listed in table 24. All scarps are west facing and are interpreted to reflect dip- or oblique-slip movement. Some scarps are formed in surficial deposits of different ages (fig. 35), which we infer to provide a maximum age for a given scarp. Except for the two scarps along profile SP7, all scarps involve unit 1 alluvial deposits (fig. 35). Profiles SP3 through SP5 are entirely on unit 1, whereas profiles SP1 and SP2 start and end on unit 1 but cross a footslope colluvial deposit (unit cf, fig. 35). Profile SP6 crosses from unit 1 to units 1 through 3. On profile SP7 (fig. 37*G*), the Fatigue Wash Fault splays into two parallel traces, along each of which is a scarp (SP7a, SP7b) formed in units 3 and 4. Interpretations regarding the relations between scarp locations and surficial deposits, and implications with respect to the timing of faulting events, are discussed below in the section entitled “Paleoseismic Interpretations from Scarp Data.”

Stratigraphy, Soils, and Age Constraints in Trenches CF1 and CF1A

Trenches CF1 and CF1A (pl. 11) expose a sequence of alluvial gravel deposits (units 1, 2, 2a, 3, 4, 4a, table 25A), colluvial wedges (units 5, 6), eolian sand (unit 8), and hybrid/transitional deposits (units 2b, 4b, 7a, 7b). Alluvial gravel and eolian sand are present on both the upthrown and downthrown blocks of the fault, but colluvial wedges only on the downthrown block. Units 1 through 4 consist of moderately well sorted to well-sorted sandy gravel with sporadic cobbly lenses (units 2a, 4a). In general, these alluvial deposits are more poorly sorted on the upthrown than on the downthrown block. Processes controlling the deposition of units 2b and 4b are uncertain. Both units have sandy- to cobbly-gravel textures, are moderately well to well sorted, and thicken close to the fault. The texture indicates an alluvial origin, whereas the thickening indicates a colluvial origin. The preferred interpretation is that these units are composed of alluvial gravel that has been eroded locally to resemble wedges. Unit 5 consists of cobbly sand, interpreted to be a proximal-debris-facies colluvial wedge (Nelson, 1992). Unit 6 consists of silty sand containing basaltic ash; the unit is interpreted to be a colluvial wedge deposited predominantly by slopewash. The unit is closely associated with a fissure fill (2, pl. 11) in the fault zone that contains abundant basaltic ash. Unit 7a is U-shaped in cross section, is present only at the fault, and is poorly sorted;

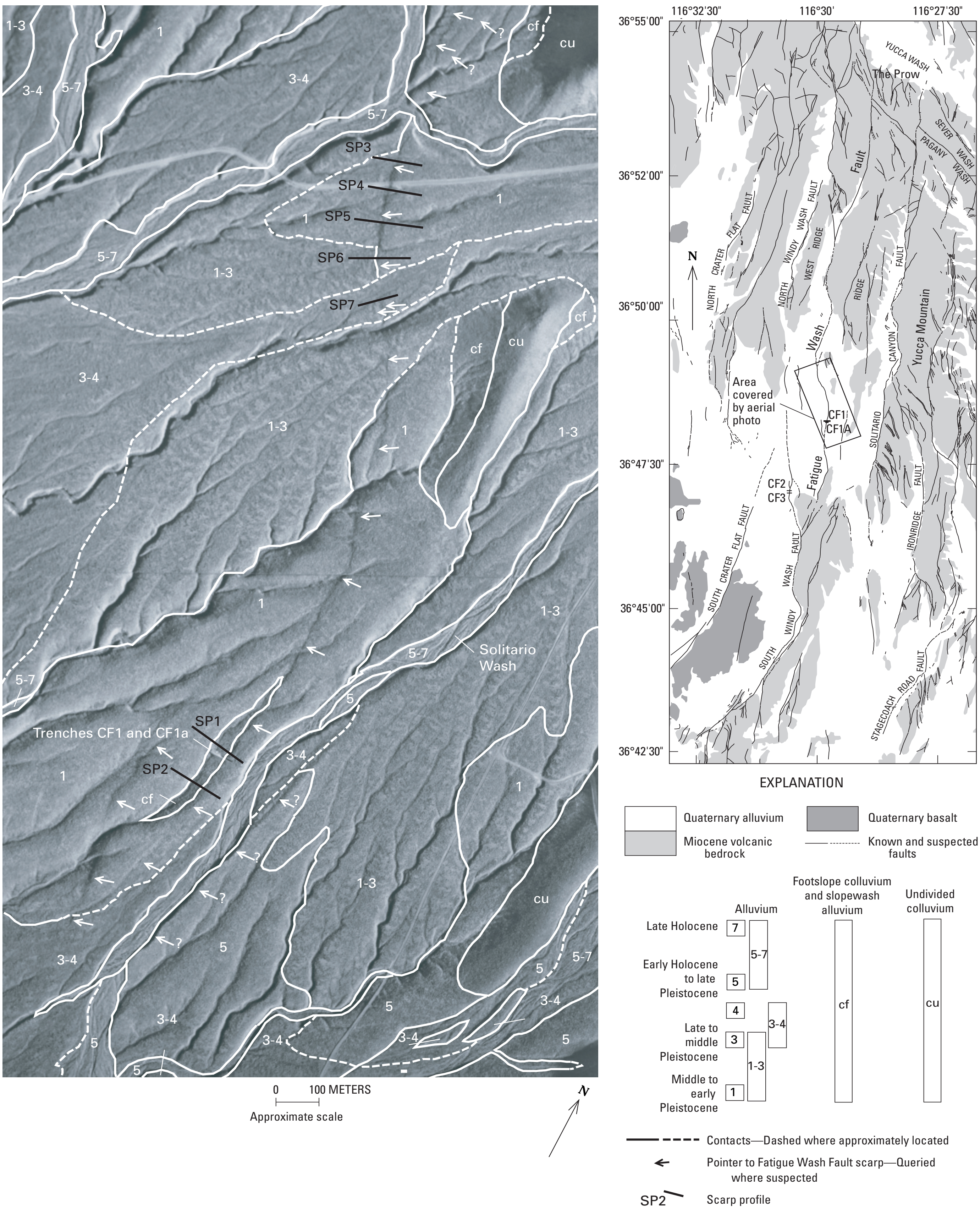

Figure 35. Distribution of surficial deposits in the vicinity of trenches CF1 and CF1A across the Fatigue Wash Fault in the Yucca Mountain area, southwestern Nevada (pl. 11; figs. 1, 2, 35), showing locations of topographic profiles SP1 through SP7 across west-facing scarp of fault.

Table 23. Numerical ages of deposits exposed in trenches CF1 and CF1A across the Fatigue Wash Fault in the Yucca Mountain area, southwestern Nevada.

[See plate 11 and figures 1, 2, and 35 for locations. Samples: TL–12 (error limit, ±2σ), thermoluminescence analysis by S.A. Mahan; HD (error limits, ±2σ), U-series analyses by J.B. Paces; TSV–386, TSV–387, U-series analyses by Szabo and O'Malley (1985); U5, U6, U-series analyses by Peterson and others (1995)]

Trench (pl. 11)	Sample	Unit and material sampled	Estimated age (ka)
CF1A	TL–12	8, buried Av soil horizon	9±1
CF1	HD 1608	1, clast rind	>401, >307
	HD 1610	5, clast rinds (inner, middle, outer)	65±4, 79±3, 325±21, 329±117, 331±10, 449±35, 447±46
	HD 1611	7, laminar K soil horizon	38±4, 172±7, 189±7
	HD 1612	7, laminar K soil horizon	102±2, 107±2, 111±1, 112±2, 116±2, 119±2, 125±1, 128±5, 169±3, 269±9
	HD 1729	5, laminar K soil horizon and clast rind	89±1, 93±1, 102±2, 115±2, 141±1
	TSV–386	Carbonate in fault-zone fill	27±3
	TSV–387	4, laminar carbonate	33±4
	U5	3, carbonate rind on clast	36±2
	U6	4, laminar horizon	60±1

Table 24. Data on topographic profiles across the west-facing scarp of the Fatigue Wash Fault near trench CF1 in the Yucca Mountain area, southwestern Nevada.

[See plate 11 and figures 1, 2, and 35 for locations and figure 36 for definitions of parameters]

Profile (fig. 37)	Surface offset (m)	Scarp height (m)	Scarp slope angle (°)
SP1	0.6	1.2	9.0
SP2	.4	1.5	9.8
SP3	.9	1.6	8.4
SP4	1.3	2.0	12.0
SP5	2.0	2.8	8.3
SP6	1.6	2.0	11.0
SP7a	.4	.8	5.2
SP7b	.2	.3	4.4

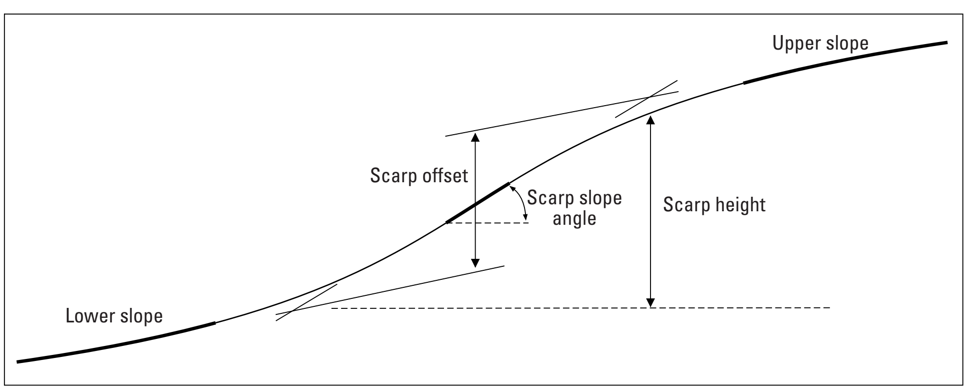

Figure 36. Schematic cross section illustrating parameters measured for topographic profiles (fig. 35; table 24). Adapted from Bucknam and Anderson (1979) and Anderson and others (1995).

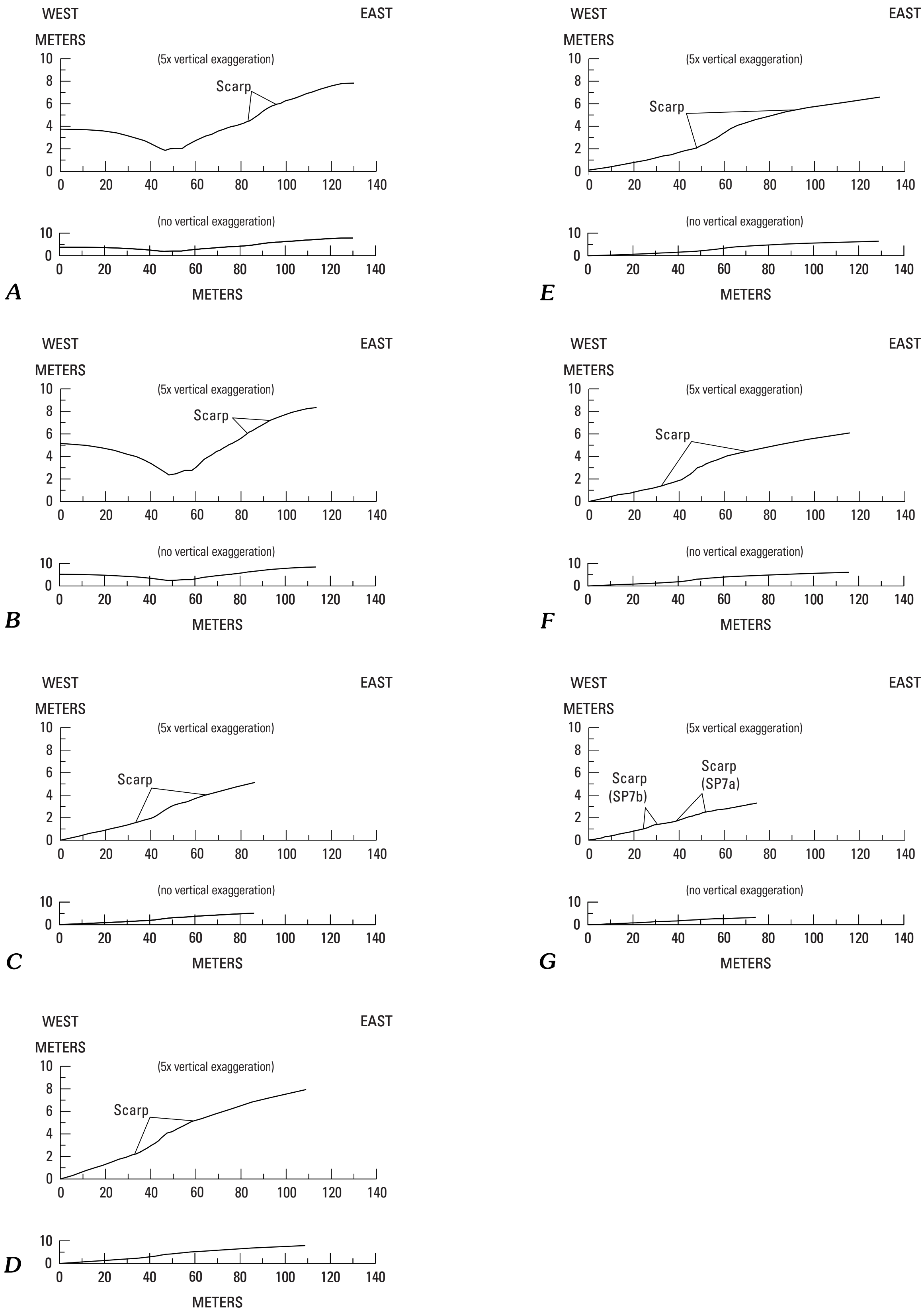

Figure 37. Topographic profiles SP1 through SP7 (*A–G*) across west-facing scarp of the Fatigue Wash Fault in the Yucca Mountain area, southwestern Nevada (pl. 11; figs. 1, 2, 35). Profile SP7 shows two discrete scarps interpreted to be two separate fault strands.

Table 25A. Summary of characteristics of lithologic units exposed in trench CF1 across the Fatigue Wash Fault in the Yucca Mountain area, southwestern Nevada.

[See plate 11 and figures 1, 2, and 35 for locations. Position: FW, footwall; HW, hanging wall. General lithology, listed in order from most to least abundant: bld, boulder; cbl, cobble; pbl, pebble; slt, silt; snd, sand. Matrix: c, coarse; f, fine; m, medium; masked, obliterated by pedogenic carbonate; pbl, pebble; slt, silt; snd, sand; vc, very coarse; vf, very fine. Cementation: CO_3, carbonate; ind, indurated; mod, moderate; non, uncemented; Si, silica; stg, strong; vstg, very strong; wk, weak. Deformation: EW_x, event wedge, with event designation; F, faulted; f, fractured; FF, fault fissure; U, unfaulted. n.a., not applicable]

Unit/ subunit	Position	General lithology	Clast size (cm)	Matrix	Cementation	Thickness (cm)	Shape	Deformation
1	FW	pbl cbl snd bld	<50	f-c snd	CO_3 mod	avg 100–>125	Tabular --------	F
2	FW	pbl cbl snd	<20	f-c pbl	CO_3 wk-mod	40–130	Lenticular tabular.	F
3	FW	pbl cbl snd w/minor bld	<40	pbl	CO_3 mod-stg	50–80	Tabular --------	F
4	FW	pbl cbl	<20	m snd	CO_3 stg	35	do ------------	F
4a	FW	pbl snd	<1	f-c snd	CO_3 mod	0–50	Lenticular	F
8	FW	snd pbl slt	<5	snd	CO_3 wk	20	Tabular --------	U
2	HW	pbl cbl snd	<40	f-m snd	CO_3 wk-mod	<160	do ------------	F
2a	HW	cbl pbl snd bld	.2–50	f-vc snd	CO_3 wk-mod	0–50	Lenticular -----	F
2b	HW	cbl pbl snd bld	.2–50	f-vc snd	CO_3 wk-mod	0–50	Wedge ---------	$EW_{w?}$, F
3	HW	pbl cbl snd	<25	snd w/minor slt	CO_3 w/Si mod-stg	60–70	Tabular --------	F
4	HW	pbl snd cbl w/minor bld	<50	f snd	CO_3 capped by Si vstg	0–100	Wedge ---------	F
4a	HW	cbl pbl snd	.2-50	f-vc snd	CO_3 mod-stg	0–30	Lenticular -----	F
4b	HW	pbl snd w/ minor cbl	<10	m snd	CO_3 mod	0–50	Wedge ---------	F
5	HW	snd cbl pbl w/minor bld slt	<30	slt-snd	CO_3 capped by Si stg	0–40	do ------------	EW_x,F
6	HW	snd pbl slt w/ minor cbl	.2–30	slt-snd	CO_3 stg	0–30	do	EW_x,F
7a	HW	snd slt pbl w/ minor cbl	<15	slt-snd	CO_3 wk	0–40	Irregular krotovina/ scour fill.	f
7b	HW	snd slt pbl w/ minor cbl	<15	slt-snd	CO_3 wk	0–30	Irregular wedge.	EW_Y, f?
8	HW	snd pbl slt	<20	slt-snd	CO_3 wk-mod	20–30	Tabular --------	f?
Shear zone	Fault zone	fines	<12	fines	CO_3 stg	max 25	Fissure---------	FF, F
Fissure fill 1	Fault zone	pbl cbl snd	<15	snd	CO_3 stg	70–100	do ------------	FF, F
Fissure fill 2 (ash)	Fault zone	pbl snd cbl slt	<10	slt-snd	CO_3 wk	10–60	do ------------	FF, f

Table 25B. Descriptions of topographic profiles across the west-facing scarp of the Fatigue Wash Fault near trench CF1 in the Yucca Mountain area, southwestern Nevada.

[See plate 11 and figures 1, 2, and 35 for locations. See table 3 for soil-horizon terminology; prefixed numbers refer to differentiated soil horizons with increasing depth, and suffixed numbers to further differentiation of properties within an individual soil horizon. Colors from Munsell Soil Color Charts (Munsell Color Co., Inc., 1992). Texture: l, loam; s, sand; slt, silt. Structure—grade: 1, weak; 2, moderate; m, massive; sg, single grain—size: c, coarse; f, fine; m, medium—type: abk, angular blocky; pl, platy; sbk, subangular blocky. Consistence—dry: eh, extremely hard; h, hard; lo, loose; sh, slightly hard; so, soft; vh, very hard—wet: po, nonplastic; so, nonsticky. CO_3 stage morphology from Birkeland (1984). Effervescence in cold dilute HCl: e, some; em, moderate; eo, none; es, strong; ev, very strong; vse, very slight. Cementation—strength: ci, indurated; cs, strong; cw, weak—type: cont, continuous; disc, discontinuous. Lower horizon boundary—distinctness: a, abrupt; c, clear; g, gradual—topography: i, irregular; s, smooth; w, wavy. Roots—abundance: 1, few; 2, common—size: f, fine; m, medium; vf, very fine—location: disp, dispersed; frc, fractures; thruout, throughout. Pores—abundance: 3, many—size: f, fine; vf, very fine—shape: thruout, throughout; v, vesicular. Rhizoliths—abundance: 1, few—size: clast, clast faces; vf, very fine. n.a., not applicable; n.o., not observed. See table 24 for data on topographic profiles]

Soil horizon	Depth (cm)	Associated unit	Color		Gravel (vol pct)	Texture	Structure	Consistence		$CaCO_3$ stage	Effervescence (HCl)	Cementation	Lower horizon boundary	Roots	Pores	Rhizoliths	Fine fraction of total (<2 mm) (vol pct)	$CaCO_3$ in fine fraction (wt pct)
			Wet	Dry				Dry	Wet									
Profile SP1																		
Avk	0	8	10YR 5/4	10YR 7/3	10	slt l	2 vf-m sbk	so	so po	n.a.	es	n.o.	a s	1 f-m thruout	3 vf-f v thruout	n.o.	n.a.	6.1
Bk	14	8	10YR 5/4	10YR 7/3	40	slt l	1 vf-f sbk	sh	so ps	I–II	em	n.o.	a w	1 vf-f disp	n.o.	n.o.	.55	7.5
2Kqmb1	17	4a	10YR 8/3	10YR 8/1	40	n.a.	m-1 f pl	eh	n.a.	IV	es-ev	ci cont CO_3	c w	n.o.	n.o.	n.o.	.16	16.4
3Kqmb1	34	4	10YR 8/2	10YR 8/1	80	n.a.	m	eh	n.a.	III+	ev	ci cont CO_3	c i	n.o.	n.o.	n.o.	.09	23.8
4Bkb1	65	3	10YR 8/3	10YR 8/1	80	n.a.	sg-1 f-m abk	lo-vh	n.a.	I–III	eo-es	cw disc CO_3	c-g w	1 vf disp	n.o.	n.o.	.18	15.1
5Bkb1	130	2	10YR 7/2	10YR 8/1	90	n.a.	sg	lo-sh	n.a.	II+	es	?cw disc CO_3	c i	1 vf-f disp	n.o.	n.o.	.21	15.9
6Bkb2	167	1	10YR 7/3	10YR 7/2	90	sl	1 vf-c abk	h	so po	II–III	ev	cs disc CO_3	n.o.	1 vf-m disp	n.o.	n.o.	.51	23.9
Profile SP2																		
Av	0	8	10YR 4/3	10YR 6/3	5	slt l	1 vf-m sbk	so	so po	n.a.	eo-vse	n.o.	c s	2 vf-co thruout	3 vf-f v thruout	n.o.	0.71	3.4
Bk1	10	8	10YR 5/4	10YR 7/3	5–10	slt l	1-2 f-vc sbk	so-sh	so po	I–II	es	n.o.	c w	2 vf-co thruout	3 vf-f v thruout	n.o.	68	6.7
Bk2	26	7	10YR 5/5	10YR 7/3	25–30	slt l	2 f-m sbk	vh	so po	II	es	n.o.	a w	1-2 vf-m disp	n.o.	n.o.	.49	9.9
2Kqmb1	35	4	10YR 7/2–7/3	10YR 8/1	50–75	n.a.	m-1 f-c sbk	eh	n.a.	IV	es-ev	ci CO_3/SiO_2 cont	c-g w	1 vf frc	n.o.	n.o.	.18	40.6
3Bkqmb1	110	3	10YR 7/3 CO_3 5/7 Si	10YR 8/1 CO_3 6/4 Si	70–80	n.a.	1 vf-c sbk	sh-vh	so po	II–III	em-es eo for SiO_2	cw-cs disc CO_3/SiO_2	c-g w	1 vf-m disp	n.o.	1 vf clast	15	11.4
4Bkb1	150	2	10YR 5/3–4	10YR 7/3–2	80	s l	sg	lo	so po	I–III–	em-es	n.o.	c-g w	1 vf-f disp	n.o.	1 vf clast	.21	12.4
5Bkb1	210	2a	10YR 7/2–7/3	10YR 8/1	– –	sls	m1m abk	so po	h-vh	II	em-es	n.o.	cw	1 vf-f disp	n.o.	1 vf clast	.12	14.1
6Bkb1	260	2	10YR 5/3–4	10YR 7/3–2	80	s l	sg	lo	so po	I–III–	em-es	n.o.	n.o.	1 vf-f disp	n.o.	1 vf clast	.23	8.9

it is interpreted to be a channel or burrow fill. Unit 7b, which is present only on the hanging wall, contains platelets of silica and carbonate from the underlying soil in a younger matrix of silty sand; the unit is interpreted as a hybrid deposit formed by both pedogenic and eolian processes.

Unit 1 is present only in the hanging wall of the Fatigue Wash Fault. Units 2 through 4 have been correlated across the fault on the basis of similar gross lithologies and sedimentologic textures, but some correlations are problematic. Unit 2, for example, consists primarily of well-sorted pebbly gravel on the downthrown block of the fault but of more poorly sorted cobbly gravel on the upthrown block immediately adjacent to the fault. In support of this correlation, unit 2 laterally grades to well-sorted pebbly gravel away from the fault on the upthrown block and to cobbly gravel near the fault on the downthrown block. The correlation of unit 4 across the fault is equally problematic because the upper part of the unit on the south wall of trench CF1 (above unit 4a on the downthrown block) is absent on the upthrown block. We interpret the missing section to have been removed by erosion, as evidenced by the unconformity between unit 8 and units 4 and 4a on the upthrown block.

Two well-developed carbonate soils are exposed on the upthrown block of the Fatigue Wash Fault in trench CF1 (pl. 11). The upper parts of the younger of these two soils (soil profile 1, pl. 11, table 25B) have a $CaCO_3$ stage III–IV morphology, and the older soil (soil horizon 6Bkb2) has up to $CaCO_3$ stage III morphology. The upper parts of both soils were stripped by erosion before deposition of the immediately overlying units; the unconformity on top of unit 1 and soil horizon 6Bkb2 is especially conspicuous. A similar sequence of soils is also present on alluvial deposits on the downthrown block (soil profile 2, pl. 11).

On the basis of observed stratigraphic and structural relations and chronology (table 23), the following interpretations and conclusions relate to the estimated ages of the deposits and soils (in ascending order) exposed in trenches CF1 and CF1A:

1. U-series estimated ages of secondary silica immediately adjacent to clasts from soil horizon 6Bkb2 (soil profile 1, south wall, trench CF1, pl. 11) indicate that this soil horizon was developed on unit 1 before 400 ka (J.B. Paces, written commun., 2000).
2. The only age obtained for units 2 and 3 is 36±2 ka (sample 1–JWB–1–YM–35–U5; sample U5, table 23), a relatively young age that likely reflects the latest cycle of silica and carbonate infiltration into these deposits rather than being a valid representation of their depositional age, which, on the basis of the ages assigned to the overlying and underlying units (unit 1, min ~400 ka; unit 4, max ~150 ka), would appear to be much older.
3. The estimated age of unit 4 is 102+42/−15 ka, based on a statistical combination of the five ages listed for sample HD 1729 (table 23). The younger ages obtained on samples TSV–387 (33±4 ka) and 1–JWB–1–YM–35–U6 (60±1 ka; sample U6, table 23) are also considered to reflect one or more late cycles of silica and carbonate infiltration that postdate the depositional age of the unit.
4. In view of the ages assigned to unit 4 below and unit 6 above, the maximum and minimum ages for unit 5 are 102+42/−15 ka and 77±6 ka (age of fissure fill 2, pl. 11), respectively. U-series analyses of silica- and carbonate-rich rinds on a boulder from unit 5 (sample HD 1610, table 23) yielded seven ages, of which only the two youngest ages (65±4 ka, 79±3 ka) are close to the maximum age of unit 6, whereas the five older ages (ranging from 325±21 to 474±46 ka) may date rind layers (intermediate and inner layers) that coated the boulder when it was part of an older deposit.
5. No ages were obtained for unit 6, at least part of which appears to have been deposited nearly contemporaneously with the development of fissure fill 2, which contains ash erupted from the nearby Lathrop Wells volcanic center (fig. 1). The age of this ash (77±6 ka) establishes a maximum age for the unit, which consists of a colluvial wedge that also contains basaltic ash. Away from the fault zone, fissure fill 2 terminates at the base of unit 6, but associated fractures continue upsection from the fissure fill through unit 6 to the base of unit 7b. A minimum age for unit 6 cannot be established, but it may be >38±4 ka (see below).
6. Ages ranging from 38±4 to 269±9 ka were obtained on materials collected from unit 7 (that is, unit 7b; samples HD 1611, HD 1612, table 23). The older ages do not appear to provide a reliable estimated depositional age, inasmuch as the unit clearly postdates the eruption of the Lathrop Wells basaltic cone (fig. 1). Also, unit 7b contains plates of older carbonate-cemented soil reworked upward into an eolian matrix that may be dated at 38±4 ka, which is the youngest age obtained on sample HD 1611. A minimum age is represented by sample TL–12, dated at 9±1 ka (see below).
7. Sample TL–12, collected from the south wall of trench CF1A (pl. 11), indicates an age of 9±1 ka for unit 8.

In terms of the standard stratigraphic sequence of surficial deposits in the Yucca Mountain area, trench unit 1 probably correlates in time with unit Qa1 (tables 2, 20), units 2 and 3 with units Qa2 and Qa3, units 4 through 6 with unit Qa3, unit 7 with unit Qa4, and unit 8 with Qa5 (see chap. 2; fig. 3). A discrepancy exists between the age of unit 4 (102+42/−15 ka, equivalent to unit Qa3), exposed on the upthrown block of the fault (pl. 11), and that of unit Qa1 (early to middle Pleistocene), mapped on the upthrown block at the surface (fig. 35)—that is, our trench data indicate that in the immediate vicinity of the fault there is a surficial mantle equivalent in age to unit Qa3. We believe that this mantle exists, but because of its limited extent, it cannot be discriminated on the aerial photograph in figure 35.

Structure Exposed in Trenches CF1 and CF1A

The main fault zone in trench CF1 (fig. 35) ranges from about 35 to 140 cm in width and is characterized by two fissure fills and a shear zone engulfed with carbonate (pl. 11). The main fault zone strikes N. 10° E. and dips from

80° E. to 80° W. The carbonate shear zone is primarily in the upthrown block and is probably the progressive result of multiple faulting events. The oldest fissure fill (1, pl. 11) consists of cobbly sand containing preferentially aligned clasts indicative of filling processes. The fissure fill, which truncates units 2, 3, 4, and 4a on the downthrown block, appears to contain a small amount (<1 volume percent) of basaltic ash when viewed under a binocular microscope, but the ash is not readily visible in the trench exposure. This older fissure fill is truncated by a more conspicuous fissure fill (2, pl. 11) containing as much as 40 volume percent basaltic ash, with a Th content of 7.2 ppm, consistent with that of ash deposits originating from the Lathrop Wells basaltic cone (fig. 1; J.B. Paces, written commun., 1995). Fissure fill 2 terminates at the base of unit 6 (north and south walls of trench CF1, pl. 11), above which are zones of vertical extension fractures continuing upward to the base of unit 7b or 8 on the hanging wall, although the fracturing relations are difficult to interpret in detail because of dense accumulations of secondary carbonate.

Units 2, 3, 4, and 4a on the downthrown block are back-rotated by the main fault zone about 5°–8° down to the east (trench CF1, pl. 11), and units 3 and 4 also are locally tilted toward the fault on the upthrown block; all the units appear to be rotated by the same amount. Away from the fault zone on both the upthrown and downthrown blocks, these units slope 3°–5° W., indicating that 8°–13° of backrotation has taken place on the downthrown block since the deposition of unit 4. No obvious fracture or fault that may have resulted from this backrotation is exposed on the downthrown block. One possible candidate is the fracture exposed closest to the west end of trench CF1. This fracture is at the position where the units begin to “roll over” (change dip direction) toward the fault, but it appears to be extensional; however, shear displacement may have occurred at depth.

Several sets of extension fractures, in addition to or including some of those discussed above, can be defined on the basis of their distinct stratigraphic levels of termination (pl. 11). Fractures in the first and oldest set terminate at the top of unit 1 on the upthrown block. Fractures in the second set, which includes only two poorly defined members, terminate between the base and middle of unit 4 on the downthrown block. Fractures in the third set terminate at the top of unit 4 (also the youngest carbonate soil horizon) on the downthrown block. Several fractures in this set “flower,” or split into multiple splays, near the top of unit 4. Two faulting events are indicated by early shear and late extensional movement along one of the fractures in this set—that is, the third fracture from the west end of trench CF1 (on the south wall) underwent early shear movement that displaced unit 2a before the deposition of unit 3, and then had later extensional deformation that cut units 3 and 4. Fractures in the fourth set, which is poorly defined with only three members exposed in trench CF1A, terminate at the base of unit 6. The fifth and youngest set is represented by questionable fractures in units 7b and 8 (fig. 38).

Paleoseismic Interpretations from Trench Data

Trench data provide evidence which is interpreted to indicate that five or more surface-rupturing paleoearthquakes have occurred on the Fatigue Wash Fault since the middle Pleistocene. Vertical displacements resulting from individual faulting events (as measured at the fault and not corrected for tilting or rotation) range from 0 to 63 cm (table 26). The sequence of faulting events (Z to pre-V), as well as other possible events, is characterized below in order from youngest to oldest. We estimate vertical displacements and, where available, net cumulative displacement after restoration of locally tilted units. Because of the steep dip of the fault, the vertical displacements are nearly the same as dip-slip displacements. Net cumulative displacement is not estimated for individual faulting events, but the total net cumulative displacement is used to calculate slip rates.

Event Z

Questionable fracturing of units 7b and 8 (fig. 38) in trench CF1A (pl. 11), with a maximum date of <9±1 ka (sample TL–12, table 23), is interpreted to represent the latest paleoseismic event (Z) on the Fatigue Wash Fault. Such an event may correlate with the latest faulting event observed on the nearby Windy Wash Fault, which is dated at 3–2 ka (see chap. 9).

Event Y

The youngest faulting event (Y) observed in trenches CF1 and CF1A (pl. 11; fig. 35) is evidenced by the down-to-the-west displacement of unit 6. Additional evidence is provided by fractures that terminate at the base of unit 7b (for example, see log of south wall of trench CF1, pl. 11). Event Y thus postdates the deposition of unit 6 and predates the deposition of unit 7b. The relation of unit 6 to unit 7a, however, is problematic. Our interpretation is that a scarp was created and served as a zone of weakness, which was then utilized by a fluvial channel and (or) a burrowing animal, resulting in the deposition of unit 7a. Fractures in that unit also terminate at the base of unit 7b (fig. 38). Although a major influx of carbonate into the Fatigue Wash Fault zone has been dated at 27±3 ka (sample TSV–386, table 23; south wall of trench CF1, pl. 11), this carbonate rind is interpreted to represent an older deposit because of the fracture relations just described. Unit 7b, as well as the lower part of unit 8, may reflect post-event Y aggradation on the downthrown block; only the upper part of unit 8 is present on the upthrown block.

The estimated displacement of unit 6 (and underlying units) by event Y is based on the assumption that the top of unit 6 was once at the same elevation as the top of unit 4a on the upthrown block. The tops of units 4a and 6 (pl. 11) are also

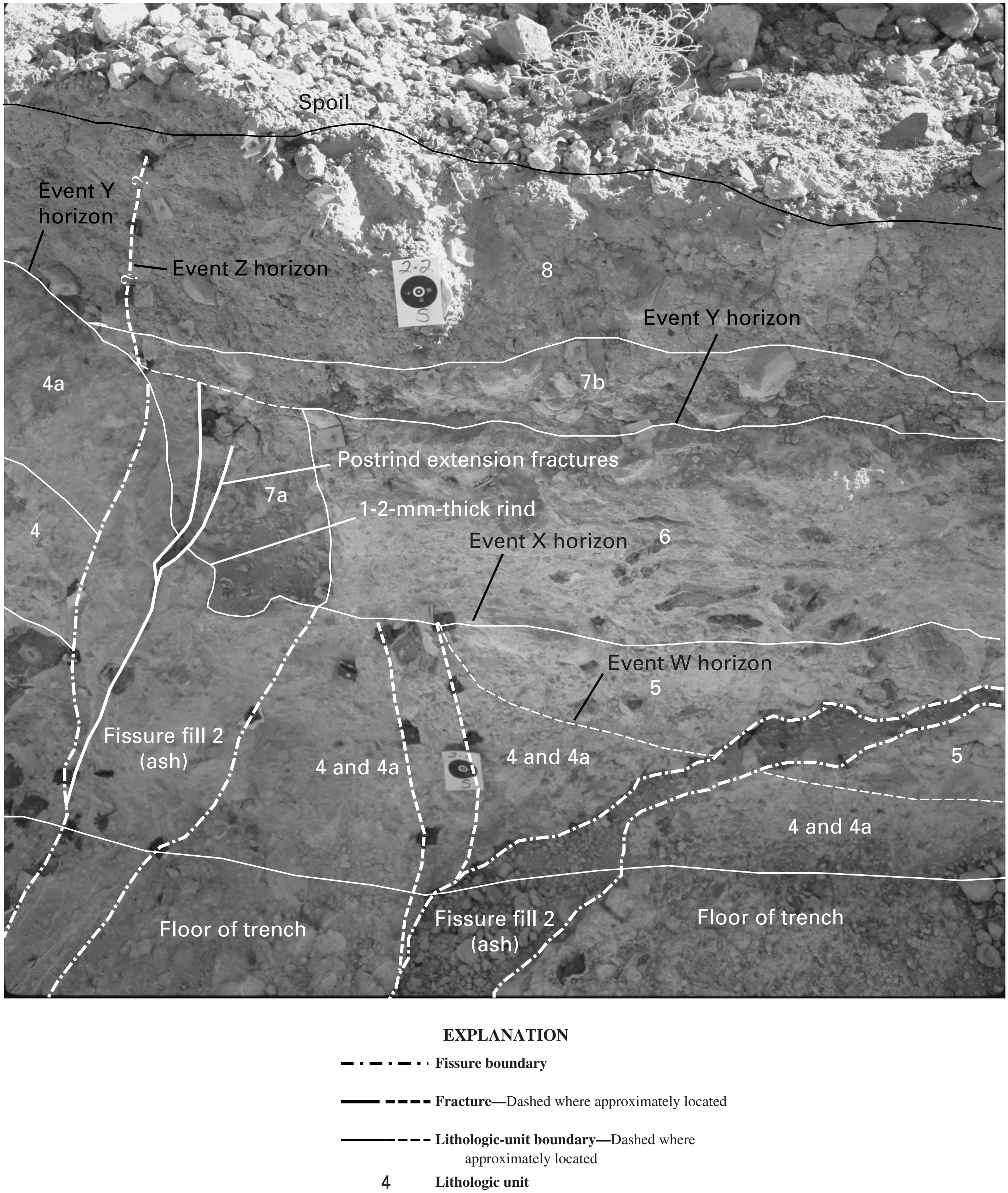

Figure 38. Stratigraphic units and faulting-event horizons exposed on south wall of trench CF1A across the Fatigue Wash Fault in the Yucca Mountain area, southwestern Nevada (pl. 11; figs. 1, 2, 35). Dark spots along some lines are markers that were emplaced to facilitate mapping.

Table 26. Estimated vertical displacements on the Fatigue Wash Fault in trenches CF1 and CF1A in the Yucca Mountain area, southwestern Nevada.

[See plate 11 and figures 1, 2, and 35 for locations. Event horizons are shown in figures 38 and 39. All values are west-side-down displacement unless otherwise noted; minimum (min), maximum (max), and preferred (pref) values are considered most reasonable because they take into account measurement error and uncertainties in locations of contacts. ?, stratigraphic constraints not available]

Event	Event horizon (figs. 38, 39	Dip (vertical) displacement (cm)												Best estimate of dip (vertical) displacement (cm)	Evidence	Comments
		South wall, trench CF1			North wall, trench CF1			South wall, trench CF1A			North wall, trench CF1A					
		min	max	pref	min	max	pref	min	max	pref	min	max	pref			
Z	Top of unit 7a (possibly as high as unit 8).	0	0	0	0	0	0	0	0	0	0	0	0	0	Questionable fractures that terminate in trench units 7b and 8.	No shear displacement observed along fractures in trenches. Event occurred after deposition of unit 7a.
Y	Top of unit 6.	11	28	18	13	28	21	11	30	24	7	52	35	25±10	Down-to-the-west displacement of massive carbonate soil (top of unit 4a on footwall to top of unit 6 on hanging wall); fractures that terminate at top of units 6 and 7a on the hanging wall.	Event occurred after deposition of unit 6, development of most of the massive carbonate soil (b1).
X	Base of unit 6.	32	?	32	42	?	42	33	?	33	25	?	25	42	Development of fissure fill 2, containing basaltic ash, and nearly contemporaneous deposition of unit 6.	Maximum thickness of unit 6 used for preferred displacement value.
W	Base of unit 5.	44	?	44	63	?	63	35	?	35	37	?	37	63	Deposition of unit 5, a colluvial wedge, and development of fissure fill 1; fractures that terminate at top of unit 4.	Maximum thickness of unit 5 used for preferred displacement value.
V	Base of unit 2b.	[1]19	?	35	0	?	63	?	?	?	?	?	?	54	Down-to-the-east displacement of unit 2a on fault just east of soil profile II on the south wall of trench CF1. Top of unit 2 at this site is not displaced. Change in sorting of unit 2 across main fault. Possible wedge deposit (unit 2b at main fault in trench CF1, pl. 11; fig. 39).	Event occurred during deposition of unit 2. Preferred separation calculated by using maximum height of unit 2b at the fault, minus any down-to-the-east separation of unit 2a just east of soil profile II. Maximum thickness of unit 2b minus down-to-the-east displacement used for preferred displacement value.
Pre-V deformation	Top of unit 1.	?	?	?	?	?	?	?	?	?	?	?	?	?	Multiple fractures that terminate at the top of unit 1 on the footwall.	Evidence for distinguishing individual events and associated displacements not observed.

[1]Down-to-the-east-displacement.

at the top of the youngest carbonate soil. A down-to-the-west step on top of this soil is clearly visible at the fault in all four trench-wall exposures. The preferred vertical distance (measured at four trench walls) of this step ranges from 18 to 35 cm (table 26). Our preferred vertical displacement for event Y at the trench sites is 25±10 cm. Event Y is dated between the age of fissure fill 2 (77±6 ka) and the age of unit 7b, which may be as old as 38±4 ka.

Event X

Evidence for event X consists of the development of fissure fill 2 (pl. 11; fig. 39), which contains abundant basaltic ash (max 40 volume percent), and the nearly contemporaneous deposition of parts of unit 6, which also contain basaltic ash, as a sedimentary wedge on the downthrown side of the fault. As stated earlier, segments of the fissure fill terminate at the base of unit 6, but poorly defined fractures continue upward through the unit. Displacement caused by event X is considered to be commensurate with the thickness of unit 6 as measured on the various trench walls. On the basis of these measurements, our best estimate of the vertical displacement caused by event X is 42 cm (table 26). The basaltic ash in fissure fill 2 has been dated at 77±6 ka (Heizler and others, 1999), which is considered to closely represent the date of event X.

Event W

Fissure fill 1 (pl. 11; fig. 39), deposition of a coarse-grained alluvial wedge (unit 5), and a well-defined set of extension fractures terminating at the base of unit 5 all provide evidence for the next-older surface-rupturing event (W) on the Fatigue Wash Fault. On the basis of measurements of the thickness of unit 5 in trenches CF1 and CF2 (fig. 35), the preferred vertical displacement is 63 cm (table 26). Given that unit 5 was deposited before fissure fill 2, the minimum date of event W is >77±6 ka, and the maximum date is <102+42/−15 ka, which is the age assigned to underlying unit 4.

The offset of trench units 2 through 4 (pl. 11; fig. 39), as observed in trenches CF1 and CF1A (fig. 35), reflects the combined effect of events W through Y. The total estimated displacement resulting from these faulting events is represented by the thicknesses of units 5 and 6, the down-to-the-west step at the top of unit 6, and the estimated thickness of deposits that were eroded off the top of units 4 and 4a before being buried by younger materials. This estimated thickness, however, is uncertain because the upper part of unit 4 is exposed only on the downthrown block. In view of this uncertainty, we believe that a reasonable approximation of the total displacement resulting from events W through Y is represented by the offset that is measurable by using the top of unit 3 on the walls of trench CF1 (pl. 11) as a datum. The vertical separation of this datum across the fault zone is about 1.4 m. This offset would indicate that about 10 cm of unit 4 was eroded off the upthrown block before the deposition of unit 5 (140 cm minus 130 cm for the combined thickness of units 5 and 6, and the down-to-the-west step at the top of unit 6; table 26).

Event V

Three lines of evidence are interpreted to indicate that a still-earlier faulting event (V) occurred during the deposition of unit 2 (pl. 11; fig. 39): (1) the wedge-shaped geometry of unit 2b on the north wall of the trench indicates a fault-derived unit (see Nelson, 1992); (2) the sorting of unit 2 changes drastically from the upthrown block, where it ranges in composition from well-sorted pebbly gravel to poorly sorted cobbly gravel, to the downthrown block, where it consists of well-sorted pebbly gravel interbedded with coarse lenses of channel gravel; and (3) one of the coarse lenses on the downthrown block is offset antithetically, down to the east, whereas the top of unit 2 directly above the lens shows no offset. On the basis of the maximum height of unit 2b minus the down-to-the-east displacement along the fracture near the west end of the trench, our best estimate for the vertical displacement from event V is 54 cm. The timing of this event is constrained between the minimum age of unit 1 (~400 ka) and the estimated age of unit 4 (102+42/−15 ka).

Pre-Event V Deformation

Multiple fractures that terminate at the top of unit 1 are evidence of a possible older event(s) exposed by trench CF1 (pl. 11; fig. 35). Because unit 1 is not exposed on the downthrown block, displacement caused by pre-event V deformation is indeterminable. Such an event(s) is dated at older than 400 ka.

Paleoseismic Interpretations from Scarp Data

As discussed above, the seven scarps that were studied along the trace of the Fatigue Wash Fault (fig. 35) were not all formed in the same surficial deposits. The latest faulting event recorded by any of the scarps is along profile SP7 (fig. 37*G*), where two small scarps (7a, 7b, table 24) on separate fault strands involve units 3 and 4 (fig. 35). The latest faulting event represented by these scarps thus postdates the deposition of this unit and so may be younger than at least the minimum age of unit 3 (34 ka; see chap. 2; fig. 3) and, possibly, even the minimum age of unit 4 (17 ka). Correlations of these surficial deposits with units exposed in trenches CF1 and CF1A (pl. 11; fig. 35) indicate a temporal equivalence with either unit 6 or unit 7b, or both. Although the evidence is equivocal, our preferred interpretation is that the 0.2-m offset on profile SP7b reflects event Z and the 0.4-m-offset on profile SP7a reflects both event Z and, possibly, event Y and (or) older faulting events.

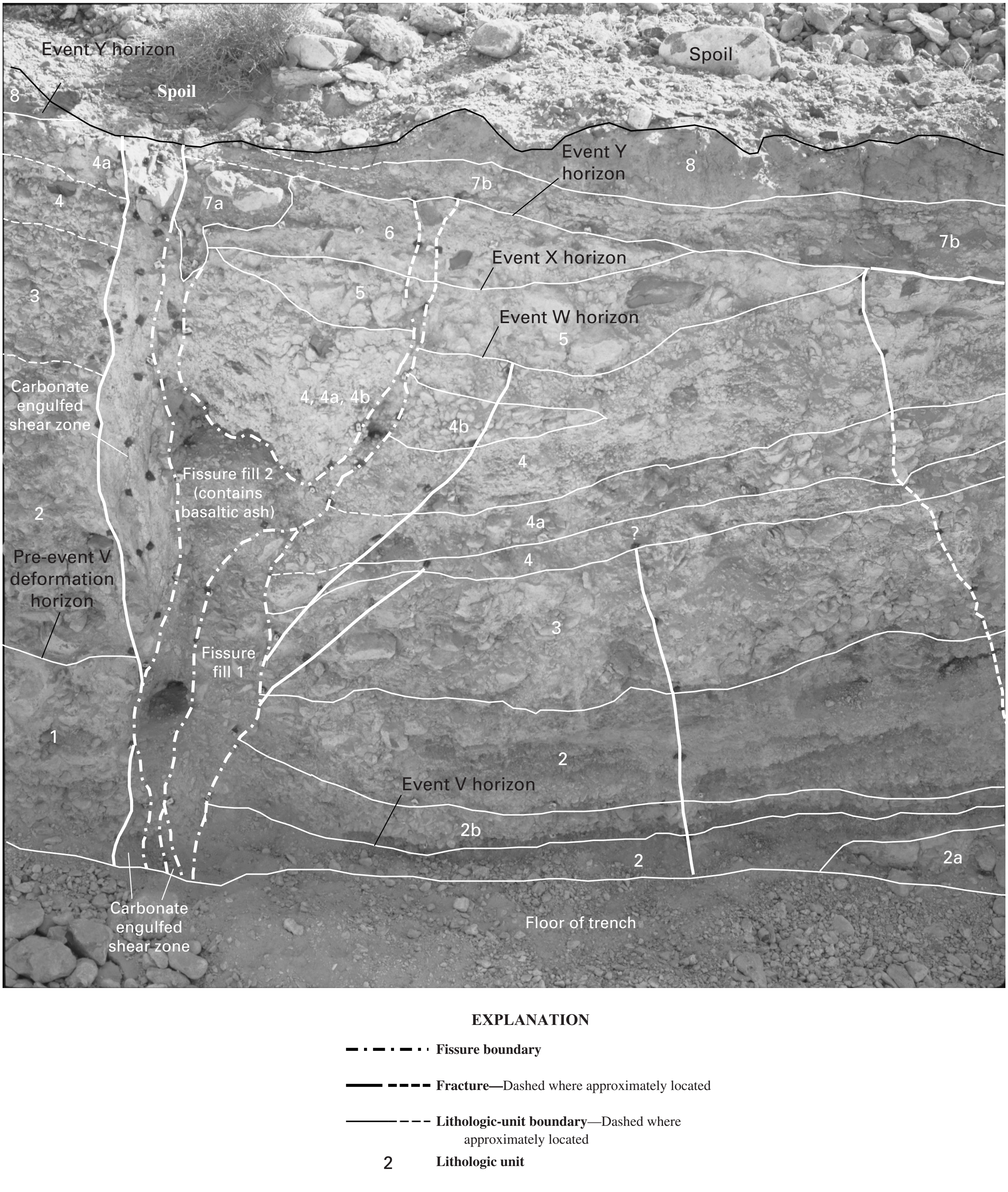

Figure 39. Stratigraphic units and faulting-event horizons exposed on south wall of trench CF1 across the Fatigue Wash Fault in the Yucca Mountain area, southwestern Nevada (pl. 11; figs. 1, 2, 35). Dark spots along some lines and within fissure fill 2 are markers that were emplaced to facilitate mapping.

Evidence is also equivocal regarding the ages of offsets reflected by the scarps along profiles SP1 through SP6 (figs. 37*A*–37*F*), all of which involve surface unit 1 (profile SP6 involves units 1–3, fig. 35), which is dated at older than 400 ka. Thus, such offsets could have occurred during most or all of the faulting events recorded in trenches CF1 and CF1A, especially taking into account the larger displacements (0.9–2.0 m) recorded on profiles SP3 through SP6. The smaller offsets on profiles SP1 and SP2 as measured near the trenches on the same fault strand as profile SP7a, however, may reflect fewer faulting events.

Slip Rates and Recurrence Intervals

A slip rate for the Fatigue Wash Fault can be estimated from both fault-scarp and trench data. To determine the total net cumulative displacement of offset surfaces or stratigraphic horizons used in slip-rate calculations, both the dip- and left-oblique-slip motion of the fault must be taken into account. The dip of the main fault exposed in trench CF1 (pl. 11; fig. 35) ranges from 80° W. to 80° E. and is therefore considered to be vertical. Although no slickensides were observed in Quaternary deposits to indicate the rake of Quaternary fault movement, rakes of 14°–70° have been documented on bedrock fault planes along the northern section of the fault (Scott and Bonk, 1984; Simonds and others, 1995). We assumed a moderate rake of 45° along a vertical fault plane to determine net cumulative displacements of geomorphic surfaces and stratigraphic units for use in calculating slip rates, as discussed below. We emphasize, however, that a much broader range of slip rates would be calculated by using both the minimum and maximum rake angles (17° versus 70°).

Assuming that (1) the surface offsets measured on profiles SP3 through SP6 (figs. 37*C*–37*F*) reflect the cumulative displacement (0.9–2.0 m) of the unit 1 surface during the past 400 k.y. and (2) movement was oblique slip with a rake of 45°, the net total displacement on the Fatigue Wash Fault ranges from 1.3 to 2.8 m. Applying these values, the long-term slip rate is calculated to range from 0.003 to 0.007 mm/yr.

In trench CF1, (pl. 11; fig. 35), unit 1 is exposed only on the upthrown block, and unit 2 is discontinuous and poorly defined. Unit 3 is fairly well defined and is present on both sides of the fault, but its age is poorly established. Unit 4 is the oldest dated unit (102+42/−15 ka) and therefore is used to estimate a slip rate. The vertical offset of the base of unit 4 in trench CF1 (pl. 11) is about 1.4 m. If the backrotation of units 2 through 4 is removed, then the offset of the base of unit 4 is about 0.4 m. Based on the 0.4-m offset and a rake of 45°, the total net cumulative displacement of the base of unit 4 is about 0.6 m. The slip rate based on the net cumulative displacement (0.6 m) and the estimated maximum and minimum ages for unit 4 (102+42/−15 ka) ranges from 0.004 to 0.007 mm/yr for that time interval.

The elapsed periods (interseismic intervals) between the four latest faulting events on the Fatigue Wash Fault range from about 30 to 140 k.y.

Faulting and Volcanism

Event X is correlated with a volcanic eruption of basaltic ash that is interpreted to have originated from the Lathrop Wells basaltic cone and was deposited in fissure fill 2 (pl. 11). Additionally, basaltic ash probably related to event X on the Fatigue Wash Fault occurs in fissure fills exposed by trenches on several other faults in the Yucca Mountain area (for example, see chaps. 7, 9, 14). These relations strongly indicate a link between Quaternary volcanism and seismicity; therefore, a model linking volcanism and faulting activity should be considered as part of the tectonic history of the area.

Acknowledgments

We thank Chris Menges and Alan Ramelli for their constructive field reviews of the trench logs, as well as many helpful observations regarding the relative ages of surfaces cut by scarps north of the trenches. We gratefully acknowledge Jim Paces, Shannon Mahan, Ken Ludwig, and Beth Widmann for their geochronology work in the trenches. Helpful discussions with John Whitney, Emily Taylor, Bob Bucknam, Jim Paces, Ken Ludwig, and Chris deFontaine regarding trench and scarp data contributed greatly to this study. Chris deFontaine helped measure profile SP7 and prepared soil and lithologic descriptions. Dave Wehner provided an early set of stereophotographs of trench CF1, and Raytheon Services, Nev., provided surveying support in the trenches. Silvio Pezzopane, Chris Menges, Jim McCalpin, and Dick Keefer reviewed the manuscript.